Boundary-Layer Effects on Acoustic Transmission Through Narrow Slit Cavities

G. P. Ward,* R. K. Lovelock, A. R. J. Murray, A. P. Hibbins, and J. R. Sambles
Department of Physics and Astronomy, Electromagnetic and Acoustic Materials Group, University of Exeter, Stocker Road, Devon EX4 4QL, United Kingdom

J. D. Smith
DSTL, Porton Down, Salisbury, Wiltshire SP4 0JQ, United Kingdom
(Received 19 January 2015; published 21 July 2015)

We explore the slit-width dependence of the resonant transmission of sound in air through both a slit array formed of aluminum slats and a single open-ended slit cavity in an aluminum plate. Our experimental results accord well with Lord Rayleigh's theory concerning how thin viscous and thermal boundary layers at a slit's walls affect the acoustic wave across the whole slit cavity. By measuring accurately the frequencies of the Fabry-Perot-like cavity resonances, we find a significant 5% reduction in the effective speed of sound through the slits when an individual viscous boundary layer occupies only 5% of the total slit width. Importantly, this effect is true for any airborne slit cavity, with the reduction being achieved despite the slit width being on a far larger scale than an individual boundary layer's thickness. This work demonstrates that the recent prevalent loss-free treatment of narrow slit cavities within acoustic metamaterials is unrealistic.

DOI: 10.1103/PhysRevLett.115.044302 PACS numbers: 43.20.Mv, 43.20.Rz, 68.35.Iv

Much modern acoustic research is focused on the design of "metamaterials," materials that have properties governed by their subwavelength structure. They make possible acoustic responses not usually seen in nature, with many utilizing narrow slit cavities [1–5] as part of their design. However, most of these studies do not incorporate well known boundary-layer loss mechanisms within their models, first described by Kirchhoff [6] in the 19th century, and extended to the slit-cavity geometry by Lord Rayleigh [7,8]. Here, we study the transmission of airborne sound through slit cavities of subwavelength widths, for both a periodic array structure and a single element. We experimentally verify Rayleigh's results and find that viscous and thermal boundary-layer effects become important for slit widths far greater than, as one may naively assume, the boundary-layer thickness. This is manifested by a reduction in the effective speed of sound through the apertures, and attenuation of the transmitted signal. Our work shows how the prevalent loss-free treatment of these cavities is unrealistic.

Consider a single, open-ended cavity of length L enclosing air bounded by two infinitely wide, perfectly rigid parallel walls. Incident sound of all wavelengths will be guided by the slit cavity, with partial reflections at each end. This establishes a standing wave within the cavity, resulting in resonant enhanced transmission via a Fabry-Perot (FP)-like resonance at frequencies given by

$$f_{\mathrm{FP}} = \frac{nc}{2(L+\Delta L)}, \tag{1}$$

where n is a positive integer, c is the adiabatic speed of sound, and ΔL is a correction to the cavity length associated with end effects. To first order, an empirical form of ΔL for each end of the slit is approximately $8w/3\pi$, w being the slit width [9]. In a slit array, the end correction takes on a more complicated form that also depends on diffractive effects associated with the periodicity Λ [10], which can lead to hybridization with the FP modes to form surface-wave modes. This has been studied extensively in recent years [1–5,11–14]; however, the modal-matching models often employed, such as the one developed by Christensen *et al.* [3], do not take into account boundary-layer perturbation of the guided modes.

In the current work we explore the effect of reducing the slit width w while keeping the slit length L constant. For both the array and the single slit, the characteristic resonant frequency f'_{FP} strongly diverges from the simple FP analysis. For narrow slits, there is a significant reduction in the observed resonant frequency away from that predicted by Eq. (1), which is attributed to viscous and thermal boundary-layer effects within the air.

Kirchhoff [6] studied sound propagation through gases confined to narrow channels, constructing an analytic solution that describes waves propagating through infinitely long, circular cross-sectioned ("tube") geometries, later expanded by Lord Rayleigh [7]. They found that boundary-layer effects at a tube's walls, which arise from the viscous and thermal properties of the gas, must be accounted for. For any acoustically rigid solid material bounding a fluid cavity, the no-slip boundary condition forces the tangential particle velocity to zero at the walls [15]. This gives rise to a viscous boundary layer, having a characteristic thickness $\delta_\nu \approx \sqrt{(\nu/2\pi f)}$, where ν is the

kinematic viscosity [16]. There is also heat exchange between the fluid and the walls; hence, there is a thermal boundary layer, having its own characteristic thickness $\delta_\kappa \approx \sqrt{(\alpha/2\pi f)}$, α being the thermal diffusivity of the gas [16]. The Prandtl number $\sigma = \delta_\nu^2/\delta_\kappa^2$ ratios these lengths, and for air it is ~0.7 [17]. One might naively expect that boundary-layer effects would only become important when the tube radius is of the order of δ_ν or δ_κ, which are ~20 μm at 5 kHz (at atmospheric pressure). However, a detailed analysis of Kirchhoff's theory presented by Weston [18] showed that the wave attenuation and particle velocity across the whole tube is affected by boundary layers that only form a small fraction of the tube radius r. Tijdeman [19] presented a general model that covered all tube sizes, which Yazaki *et al.* [16] verified recently, finding experimental agreement in the predicted attenuation and phase velocity of a wave propagating through an "infinitely" long tube over 4 orders of magnitude of tube radii. A 10% reduction in the phase velocity of the pressure wave $v_p = f\lambda_0$ ($\lambda_0 =$ free space wavelength), relative to the adiabatic speed of sound c_0, is exhibited when the tube radius is roughly 10 times larger than the thickness of the thermodynamic boundary layers.

Lord Rayleigh extended Kirchhoff's solutions to the "parallel wall" (i.e., slit) geometry [7,8]. He states that Kirchhoff's tube equations are still valid for slits, with a substitution of the slit width w for the tube radius r. Stinson [20] simplified Kirchhoff's solutions when applied to tube cross sections of arbitrary shape, including an infinitely long slit cavity, finding agreement with Lord Rayleigh. More recently, Homentcovschi and Miles studied a nonresonant system of periodic, very thin screens ($L \ll \lambda_0$) with slit widths of the order of the boundary-layer thickness, investigating acoustic attenuation due to viscosity and its effect on diffraction [21,22]. However, none of this research explored the effect of the boundary-layer perturbation on a resonant slit system, which is the focus of the current study.

Figure 1 shows the experimental setup. In an array, thin aluminum slats ($d \ll \lambda_0$) of size $600 \times 2.9 \times 19.8$ mm were stacked vertically in a wooden sample holder, separated by sets of polyester spacers of sizes 0.05 ± 0.01 mm, 0.1 ± 0.01 mm, and 0.5 ± 0.03 mm, resulting in a sample area of 560×400 mm. In order to have incident sound approximate an infinite planar wave, the sample was placed between two spherical mirrors of radius 220 mm and focal length 1 m. One mirror collimated a sound signal from a Scan-Speak D2004 speaker positioned at its focal point; the other focused the sound to a Brüel and Kjær 4190 microphone. The sample was positioned such that the collimated beam was incident normal to the front face of the array of slit cavities. A Gaussian pulse containing audible frequencies was produced from the speaker, and the microphone's recorded time signal was Fourier analyzed to extract the transmitted spectra of the sample. This was normalized in the frequency domain by division of a reference signal

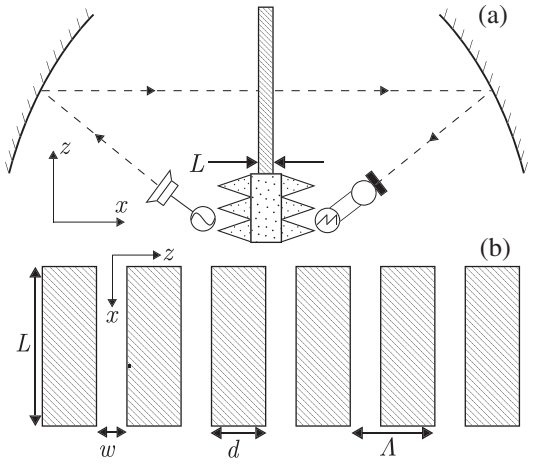

FIG. 1. (a) Schematic of the slit-array experimental configuration. The aluminum slats (hatched) were stacked vertically between two mirrors 3 m apart, with a speaker and microphone placed at their focal lengths 1 m away. The sample stand was covered in acoustic absorber (dotted fill) and the beam path is indicated by a dashed arrow. (b) Schematic of the slit-array sample itself, with dimensions labeled (not to scale). Here, $L = 19.8 \pm 0.12$ mm, $d = 2.91 \pm 0.03$ mm, and $\Lambda = d + w$.

recorded without the sample in place, and a correction was applied to account for leakage of the signal around the sample, the details of which are available in the Supplemental Material [23]. The experiment was repeated four times for each slit width, and the mean resonant frequencies were extracted from the transmission spectra by the fitting of a Lorentzian function to each peak. Error bars represent the standard deviation from these means. This process was repeated for the single slit case, with two blocks of aluminum of dimensions $202 \times 243 \times 35$ mm, as shown in Fig. 2. The only difference in the method was the lack of collimating mirrors. With only one slit in the sample, a collimated beam was not required to approximate a planar wave, and direct transmission between the receiver

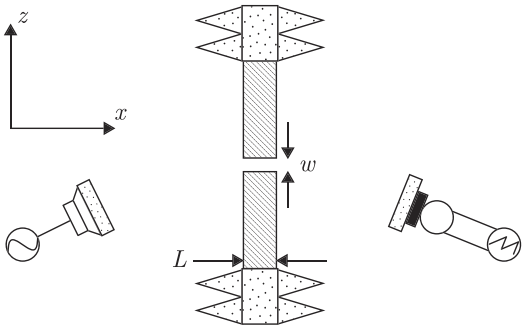

FIG. 2. Schematic of the single slit experimental configuration. The dashed blocks represent the aluminum sample, and the dotted blocks represent an acoustic baffle. The microphone and speaker are ~20° off normal in the xz plane, covered in acoustic absorber, and separated from the sample faces by 220 and 400 mm, respectively. Here, $L = 35.0 \pm 0.1$ mm.

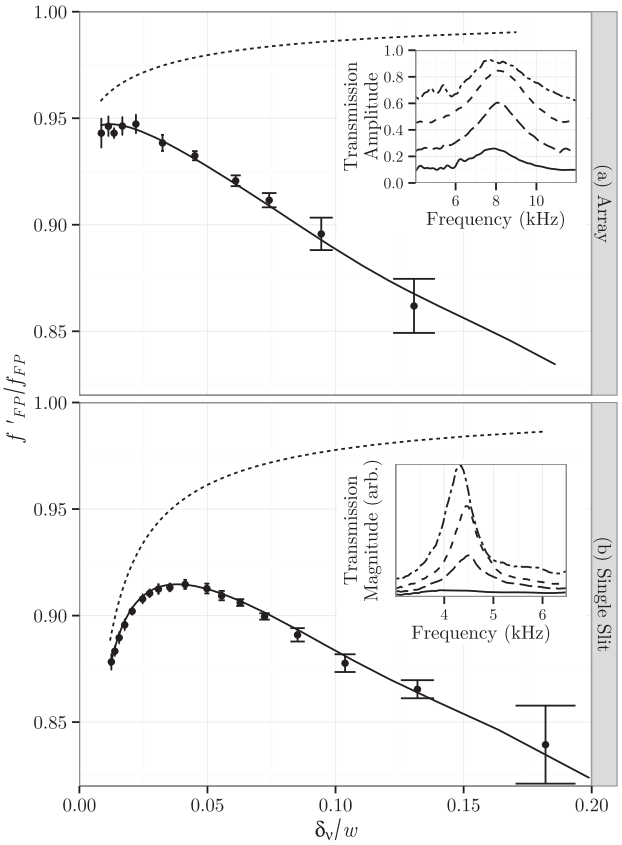

FIG. 3. The fundamental resonant frequency of each slit cavity f'_{FP}, normalized to that predicted by the Fabry-Perot condition f_{FP} as a function of the ratio of viscous boundary-layer thickness δ_ν to slit width w. The solid circles are the experimentally recorded mean frequencies, with the error bars representing their standard deviation. The dashed lines represent a lossless FEM numerical prediction, and the solid lines a more complete numerical prediction that includes the viscous and thermal properties of each system. The top and bottom panels represent the slit array and single slit samples, respectively. Insets: examples of the experimentally measured transmitted frequency spectra for the relevant sample. Four different slit widths of 2.0, 1.0, 0.5, and 0.2 mm are represented by the dot-dashed, dashed, long-dashed, and solid lines, respectively.

and detector produced significantly stronger signals. Both the microphone and speaker were tilted ~20° off the x axis and covered in absorber to weaken standing waves set up between them and the sample faces. Typical transmission spectra for both the slit array and single slit samples are shown in the insets of Fig. 3. The samples were chosen to ensure that the slit widths and array periodicities remained subwavelength to incident sound ($100w < \lambda_0 < 300w$, and $8\Lambda < \lambda_0 < 14\Lambda$), avoiding any diffractive phenomena. The measurements were taken under different temperatures, pressures, and humidities, the latter two having negligible effect [24]. A temperature change causes a small but systematic frequency shift of $1.64 \times 10^{-3}\ f\,\mathrm{Hz}^{-1}\,\mathrm{K}$ [23], and thus all data were normalized to 293.15 K. Small systematic changes in all slit widths are included to account for the fact that, for the slit array, bowing of the slats will give somewhat wider gaps than the measured spacers, while for the single slits compression of the spacers by the weight of the sample and its baffle reduced the width to below that intended. Detailed information has been provided in the Supplemental Material [23].

Figure 3 shows the ratio of the measured fundamental ($n = 1$) resonant frequency f'_{FP} of the slit cavity to that predicted by the Fabry-Perot condition (1) f_{FP}, as a function of the fraction of slit width w occupied by a viscous boundary layer δ_ν, for both the slit-array sample (top) and single slit sample (bottom). Both experimental data sets are compared with numerical data obtained from the finite element method (FEM) software COMSOL multiphysics, with and without thermal and viscous contributions. Resonant frequency uncertainties at the smallest gaps are increased due to broadening of the modes, as well as a reduction in the signal-to-noise ratio. For the array, the largest gap resonances were also significantly broader, due to a reduction in the quality factor caused by decreasing the rigid-body filling fraction w/d [12].

For gaps where $(\delta_\nu/w) < 0.03$, the trend of our data agrees with the predictions of the lossless FEM model (dashed line), which solves the acoustic wave equation. The diffractive end correction ΔL is the dominant physical mechanism shifting the resonance down in frequency in this regime, increasing with w. While not shown here we have confirmed that Christensen's lossless modal-matching model [3] agrees very well with this lossless FEM model, an example of a loss-free model typically used in modern acoustic metamaterial research. The important result for both samples is the marked deviation between the lossless models and the experiment for $(\delta_\nu/w) \geq 0.03$. To explain this, the thermal and viscous properties of the air need to be incorporated into the FEM model. This is done by utilizing the linearized Navier-Stokes equation for a viscous fluid, allowing heat transfer between the fluid and solid walls, and applying the no-slip and isothermal boundary conditions at each rigid wall. Figure 3 demonstrates good agreement between this more complete model (solid line) and the experimental data for all slit widths. Hence, on a scale more than an order of magnitude larger than the boundary-layer thickness, these thermodynamic effects are significant. Upon closer inspection, the results of the loss-free and loss-inclusive models have not converged even for the largest measured slit widths ($(\delta_\nu/w) < 0.03$).

As the slits are narrowed, the influence of the boundary layers becomes more substantial, and there is a strong reduction in the resonant frequency attributed to a decrease in the phase velocity v_p [18] (i.e., the effective speed of sound). This is because the wavelength is fixed by the FP condition (1). It is important to note that a simple bulk-loss component added to the sound velocity in air does not predict this frequency reduction, yielding only signal

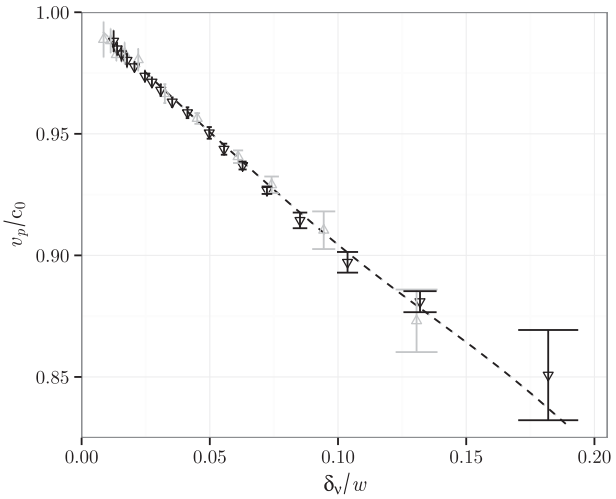

FIG. 4. Ratio of the calculated effective speed of sound v_p to adiabatic speed c_0 in each slit cavity, as a function of the ratio of viscous boundary-layer thickness δ_ν to slit width w. Triangular points and accompanying error bars are experimental data converted from Fig. 3, with black and gray representing the single slit and slit-array data, respectively. The dashed line represents the prediction of Stinson's [20] analytic theory.

attenuation for the narrowest slits. In addition, we have checked that the ratios of slit width to array periodicity w/Λ, slit width to slat width w/d, or array periodicity to incident wavelength Λ/λ do not significantly impact on the phenomena of interest.

Figure 4 shows the dependence on slit width δ_ν/w of the effective speed of sound v_p/c_0. We compare our results (triangular points) with those analytically derived by Stinson [20] (dashed line), whose simplified treatment of the slit geometry provides solutions for the wave vector $k = (2\pi/\lambda)$ of a wave traveling through an infinitely long slit of a given width at a given frequency, from which one can extract the phase velocity v_p. Application of Stinson's model to our resonant slit geometry requires the characteristic frequency f'_{FP}, which was determined from the loss-inclusive FEM model, in order to calculate the boundary-layer thickness for each slit width. To directly compare our experimental results with Stinson's prediction for v_p, we need to know the wavelength of the fundamental resonance of our slit cavities, corresponding to $2(L + \Delta L)$. This allows us to determine v_p by solving the Fabry-Perot equation (1). An estimate of ΔL that includes the effects of the viscous and thermal boundary layers can be extracted from the FEM loss-inclusive model, using the relation

$$\Delta L = L_{n=2} - 2L_{n=1}, \tag{2}$$

where $L_{n=2}$ is the length of the slit for which the $n = 2$ mode matches the resonant frequency of the fundamental $n = 1$ mode for $L_{n=1}$. Applying Eq. (2) and then fitting a polynomial to the calculated ΔL as a function of w allows one to determine an approximate ΔL for any given slit width. This was performed separately for the slit array and the single slit. For a single slit, to first order, $\Delta L = 8w/3\pi$ [9], so $\Delta L \to 0$ when $w \to 0$. For a slit array the end correction has a different form [10], but it contains a similar dependence, and also tends to zero. Thus, we were able to calculate v_p (with negligible error) for our experimental data using Eq. (1), plotted in Fig. 4.

There is very good agreement between Stinson's prediction for v_p and our data across the whole range of measured slit widths for both samples. In this regime the reduction in effective sound speed follows the same linear trend for both the slit array and single slit, confirming that it is the ratio of slit width to thermodynamic boundary-layer size that is the important parameter. For the smallest gap in the single slit case, where $\delta_\nu/w \approx 0.18$, v_p falls by nearly 15%, consistent with the results of Yazaki [16] (substituting slit width w for tube radius r) and thus verifying Lord Rayleigh's theory. Even when the size of a viscous boundary layer is only 5% of that of the whole slit, there is a significant ~5% drop in v_p, indicating that it is unwise to use an idealistic loss-free model in the design of an airborne-acoustic metamaterial.

In conclusion, the resonant transmission of sound in narrow air slits ($100w < \lambda_0 < 300w$) through both a subwavelength periodic slit array ($8\Lambda < \lambda_0 < 14\Lambda$) and a single slit cavity has been measured for a range of slit widths. It was found that slit widths an order of magnitude larger than the viscous and thermal boundary-layer thickness showed a significant reduction in resonant frequency and substantial damping of the resonance compared to the simple end-corrected Fabry-Perot condition and to lossless modal-matching models [3]. Not only does this study show that boundary-layer effects play a significant role in slit cavities where they only form a tiny fraction of the whole width (e.g., in a 1 mm air-filled slit at 5 kHz), but it also opens up new possibilities for metamaterial design. Irrespective of the solid material used, a simple rigid-walled cavity filled with air can act as a broadband absorber, and the effective speed of sound inside it can be controlled via the slit width.

The authors would like to thank DSTL for their financial support. ©Crown Copyright 2015. This was published with the permission of DSTL on behalf of the controller of HMSO.

*Corresponding author.
gpw204@exeter.ac.uk

[1] X. Zhang, Phys. Rev. B **71**, 241102 (2005).
[2] M. H. Lu, X. K. Liu, L. Feng, J. Li, C. P. Huang, Y. F. Chen, Y. Y. Zhu, S. N. Zhu, and N. B. Ming, Phys. Rev. Lett. **99**, 174301 (2007).
[3] J. Christensen, L. Martin-Moreno, and F. J. Garcia-Vidal, Phys. Rev. Lett. **101**, 014301 (2008).
[4] X. Wang, J. Appl. Phys. **108**, 064903 (2010).

[5] J. Christensen, L. Martín-Moreno, and F. J. García-Vidal, Phys. Rev. B **81**, 174104 (2010).
[6] G. Kirchhoff, Ann. Phys. (Berlin) **210**, 177 (1868).
[7] L. Rayleigh, *The Theory of Sound—Volume 2*, 2nd ed. (Macmillan, London, 1877), p. 323.
[8] L. Rayleigh, Philos. Mag. **1**, 301 (1901).
[9] L. E. Kinsler, A. R. Frey, A. B. Coppens, and J. V. Sanders, *Fundamentals of Acoustics*, 4th ed. (John Wiley & Sons, Inc., New York, 1999), Vol. 4, p. 274.
[10] F. P. Mechel and M. L. Munjal, *Formulas of Acoustics* (Springer, Berlin, 2008), pp. 408–410.
[11] B. Hou, J. Mei, M. Ke, W. Wen, Z. Liu, J. Shi, and P. Sheng, Phys. Rev. B **76**, 054303 (2007).
[12] H. Estrada, P. Candelas, A. Uris, F. Belmar, F. Meseguer, and F. J. Garcia de Abajo, Appl. Phys. Lett. **93**, 011907 (2008).
[13] B. Hou, J. Mei, M. Ke, Z. Liu, J. Shi, and W. Wen, J. Appl. Phys. **104**, 014909 (2008).
[14] H. Estrada, P. Candelas, A. Uris, F. Belmar, F. Meseguer, and F. J. García de Abajo, Wave Motion **48**, 235 (2011).
[15] L. E. Kinsler, A. R. Frey, A. B. Coppens, and J. V. Sanders, *Fundamentals of Acoustics*, 4th ed. (John Wiley & Sons, Inc., New York, 1999), Vol. 1, p. 229.
[16] T. Yazaki, Y. Tashiro, and T. Biwa, Proc. R. Soc. B **463**, 2855 (2007).
[17] L. E. Kinsler, A. R. Frey, A. B. Coppens, and J. V. Sanders, *Fundamentals of Acoustics*, 4th ed. (John Wiley & Sons, Inc., New York, 1999), Vol. 1, p. 217.
[18] D. E. Weston, Proc. Phys. Soc. London Sect. B **66**, 695 (1953).
[19] H. Tijdeman, J. Sound Vib. **39**, 1 (1975).
[20] M. R. Stinson, J. Acoust. Soc. Am. **89**, 550 (1991).
[21] D. Homentcovschi, R. N. Miles, and L. Tan, J. Acoust. Soc. Am. **117**, 2761 (2005).
[22] D. Homentcovschi and R. N. Miles, Wave Motion **45**, 191 (2008).
[23] See Supplemental Material at http://link.aps.org/supplemental/10.1103/PhysRevLett.115.044302 for more details on the experimental method.
[24] O. Cramer, J. Acoust. Soc. Am. **93**, 2510 (1993).